TRB

TRANSPORTATION RESEARCH RECORD

Journal of the Transportation Research Board No. 1919

Rigid and Flexible Pavement Design 2005

TRANSPORTATION RESEARCH BOARD
OF THE NATIONAL ACADEMIES

TRB

TRANSPORTATION RESEARCH RECORD

Journal of the Transportation Research Board, No. 1919

Rigid and Flexible Pavement Design 2005

A Peer-Reviewed Publication

TRANSPORTATION RESEARCH BOARD
OF THE NATIONAL ACADEMIES

Washington, D.C.
2005

www.TRB.org

Transportation Research Record 1919
ISSN 0361-1981
ISBN 0-309-09392-9

Subscriber Category
IIB pavement design, management, and performance

Printed in the United States of America

Sponsorship of Transportation Research Record 1919

DESIGN AND CONSTRUCTION GROUP
Gale C. Page, Florida Department of Transportation (Chair)

Pavement Management Section
Nicolaas F. Coetzee, Dynatest Consulting, Inc. (Chair), Judith B. Corley-Lay, Gary E. Elkins, Kenneth W. Fults, Mark P. Gardner, Anastasios M. Ioannides, Thomas J. Kazmierowski, Joe P. Mahoney, Roger C. Olson, James C. Wambold

Rigid Pavement Design Committee
Anastasios M. Ioannides, University of Cincinnati (Chair), Jose Tadeu Balbo, Ernest J. Barenberg, Judith B. Corley-Lay, James A. Crovetti, Mostafa Elseifi, Kathleen T. Hall, Michael I. Hammons, Jacob Hiller, Andrew M. Johnson, Lev Khazanovich, Francesca La Torre, David L. Lippert, Andreas Loizos, Robert R. Long, Jr., Aramis Lopez, Jr., James W. Mack, B. Frank McCullough, J. P. Mohsen, Tatsuo Nishizawa, Linda M. Pierce, David W. Pittman, Chetana Rao, Robert Otto Rasmussen, Jeffery R. Roesler, Dulce Rufino, Larry A. Scofield, Kurt D. Smith, Shiraz D. Tayabji, Julie M. Vandenbossche, Gerald F. Voigt, Thomas D. White, Sameh M. Zaghloul

Flexible Pavement Design Committee
Kenneth W. Fults, Round Rock, Texas (Chair), Sirous H. Alavi, Gilbert Y. Baladi, Fouad M. Bayomy, Bjorn Birgisson, Albert J. Bush III, Trenton M. Clark, Judith B. Corley-Lay, Bruce Dietrich, Fred N. Finn, Kevin D. Hall, Mustaque Hossain, Andrew M. Johnson, Jiwon Kim, Fenella M. Long, Michael S. Mamlouk, Richard W. May, Walid M. Nassar, David E. Newcomb, Katherine A. Petros, Stephen B. Seeds, Peter J. Stephanos, Marshall R. Thompson, David H. Timm, Per Ullidtz, Harold L. Von Quintus, Kim A. Willoughby, Haiping Zhou

Sponsorship is indicated by a footnote at the end of each paper. The organizational units, officers, and members are as of December 31, 2004.

Transportation Research Board Staff
Stephen F. Maher, Engineer of Design
Michael DeCarmine, Senior Program Associate

Publications Office
Chrysa Cullather, Editor; Mark Farrell, Production Editor;
Mary McLaughlin, Proofreader; Carole O'Connor, Manuscript Preparer

Ann E. Petty, Managing Editor; Juanita Green, Production Manager;
Phyllis Barber, Publishing Administrator; Jennifer J. Weeks, Manuscript Preparation Manager

Transportation Research Record 1919

Contents

PART 2—FLEXIBLE PAVEMENTS

TRANSPORTATION RESEARCH BOARD
500 Fifth Street, NW
Washington, DC 20001

ADDRESS SERVICE REQUESTED

TRB

TRANSPORTATION RESEARCH RECORD

Journal of the Transportation Research Board, No. 1919

Rigid and Flexible Pavement Design 2005

A Peer-Reviewed Publication

TRANSPORTATION RESEARCH BOARD
OF THE NATIONAL ACADEMIES

Washington, D.C.
2005

www.TRB.org

Transportation Research Record 1919
ISSN 0361-1981
ISBN 0-309-09392-9

Subscriber Category
IIB pavement design, management, and performance

Printed in the United States of America

Sponsorship of Transportation Research Record 1919

DESIGN AND CONSTRUCTION GROUP
Gale C. Page, Florida Department of Transportation (Chair)

Pavement Management Section
Nicolaas F. Coetzee, Dynatest Consulting, Inc. (Chair), Judith B. Corley-Lay, Gary E. Elkins, Kenneth W. Fults, Mark P. Gardner, Anastasios M. Ioannides, Thomas J. Kazmierowski, Joe P. Mahoney, Roger C. Olson, James C. Wambold

Rigid Pavement Design Committee
Anastasios M. Ioannides, University of Cincinnati (Chair), Jose Tadeu Balbo, Ernest J. Barenberg, Judith B. Corley-Lay, James A. Crovetti, Mostafa Elseifi, Kathleen T. Hall, Michael I. Hammons, Jacob Hiller, Andrew M. Johnson, Lev Khazanovich, Francesca La Torre, David L. Lippert, Andreas Loizos, Robert R. Long, Jr., Aramis Lopez, Jr., James W. Mack, B. Frank McCullough, J. P. Mohsen, Tatsuo Nishizawa, Linda M. Pierce, David W. Pittman, Chetana Rao, Robert Otto Rasmussen, Jeffery R. Roesler, Dulce Rufino, Larry A. Scofield, Kurt D. Smith, Shiraz D. Tayabji, Julie M. Vandenbossche, Gerald F. Voigt, Thomas D. White, Sameh M. Zaghloul

Flexible Pavement Design Committee
Kenneth W. Fults, Round Rock, Texas (Chair), Sirous H. Alavi, Gilbert Y. Baladi, Fouad M. Bayomy, Bjorn Birgisson, Albert J. Bush III, Trenton M. Clark, Judith B. Corley-Lay, Bruce Dietrich, Fred N. Finn, Kevin D. Hall, Mustaque Hossain, Andrew M. Johnson, Jiwon Kim, Fenella M. Long, Michael S. Mamlouk, Richard W. May, Walid M. Nassar, David E. Newcomb, Katherine A. Petros, Stephen B. Seeds, Peter J. Stephanos, Marshall R. Thompson, David H. Timm, Per Ullidtz, Harold L. Von Quintus, Kim A. Willoughby, Haiping Zhou

Sponsorship is indicated by a footnote at the end of each paper. The organizational units, officers, and members are as of December 31, 2004.

Transportation Research Board Staff
Stephen F. Maher, Engineer of Design
Michael DeCarmine, Senior Program Associate

Publications Office
Chrysa Cullather, Editor; Mark Farrell, Production Editor;
Mary McLaughlin, Proofreader; Carole O'Connor, Manuscript Preparer

Ann E. Petty, Managing Editor; Juanita Green, Production Manager;
Phyllis Barber, Publishing Administrator; Jennifer J. Weeks, Manuscript Preparation Manager

Transportation Research Record 1919

Contents

Predicting Asphalt Pavement Temperature with a Three-Dimensional Finite Element Method

Manuel J. C. Minhoto, Jorge C. Pais,
Paulo A. A. Pereira, and Luis G. Picado-Santos

A three-dimensional (3D) finite element (FE) model was developed to calculate the temperature of a pavement located in northeast Portugal. A case study was developed to validate the model. Input data to the model were the hourly values for solar radiation and temperature and mean daily values of wind speed obtained from a meteorological station. The thermal response of a multilayered pavement structure was modeled with a transient thermal analysis for 4 months (December 2003 to April 2004), and the analysis was initiated with the full-depth constant initial temperature obtained from field measurements. During these 4 months, the pavement temperature was measured at a new pavement section, located in IP4 main road, near Bragança, in northern Portugal. At this location, seven thermocouples were installed in the asphalt concrete layers at seven different depths. These pavement data were used to validate this simulation model by a comparison of model calculated data with measured pavement temperatures. The 3D FE analysis proved to be an interesting tool to simulate the transient behavior of asphalt concrete pavements. The suggested simulation model can predict the pavement temperature at different levels of bituminous layers with good accuracy.

Bituminous overlays have been the most common method of pavement rehabilitation. In an overlay placed on a cracked pavement, the cracks will develop and propagate to the pavement surface directly above cracks in the existing pavement under static and repetitive loading during the first few years of service. This mode of distress is traditionally referred to as "reflective cracking" and is a major concern to highway agencies throughout the world. Thus, the asphalt concrete overlay is exposed to great strains and stresses when subjected to traffic and thermal loadings. Several authors (*1, 2*) suggest different mechanisms as the origin and propagation of cracks in overlays of pavements:

1. Thermal stresses from thermal fatigue occur when temperature variations induce cyclic openings and closures of cracks in the pavement, which induce stress concentrations in the overlay.
2. Thermal stresses result from rapid cooling of the top layer, which induces critical tensile stresses on overlay.
3. Repetitive traffic loads induce additional distress in the overlay and increase the rate of crack propagation, whether or not these cracks originate from thermal stresses.
4. Compressive stresses or strains occur at the top of the unbound materials, when the failure mechanism is likely to be something other than reflective or fatigue cracking.

The literature review (*2*) also revealed that daily and seasonal temperature variations, as well as the associated thermal stresses, could be a cause of premature overlay cracking, which affects the predictive overlay service life of asphalt concrete (AC) layers. In regions that experience large daily temperatures variations or extremely low temperatures, the thermal conditions play a major role in reflective cracking response of a multilayered pavement structure. On the one hand, binder properties (e.g., stiffness, ageing, penetration) are sensitive to temperature variations. On the other hand, the combination of the two most important effects—wheel loads passing above (or near) the crack and the tension increase in the material above the crack (in the overlay) because of rapidly decreasing of temperatures—have been identified as the most likely causes of high states of stress and strain above the crack and is most likely responsible for the reflective cracking (*3*).

Daily temperature variations have an important influence on the pavement thermal state at a depth of a few decimeters below the surface. Depending on the temperature variation level, stresses are induced in the overlay in two different ways, which need to be distinguished: through restrained shrinkage of the overlay and through the existing movements of slabs caused by the thermal shrinking phenomenon.

To calculate the pavement thermal effects and the thermal response of the AC mixes, it is necessary to evaluate the temperature distribution evolution on many depths of bituminous layers throughout typical 24-h periods. The temperature distributions obtained for different hours during the day allow for the calculation of thermal effects in the zone above the crack; they can be used to investigate other effects, such as the temperature influence on properties of layer materials (like stiffness).

The time variation of pavement thermal state is controlled by climatic conditions, thermal diffusivity of the materials, thermal conductivity, specific heat, density, and the depth below the surface (*2, 4*). The temperature distribution on a pavement structure can be obtained through field measurements using temperature-recording equipment (Datalogger associated with thermocouples) or can be estimated by using mathematical models. The option of using the field measurement is desirable because actual temperature can be reliably measured and used in stress calculation models. However, this method is relatively

M. J. C. Minhoto, Superior School of Management and Technology, Bragança Polytechnic Institute, Campus de Santa Apolonia, Apartado 134, 5301-857 Bragança, Portugal. J. C. Pais and P. A. A. Pereira, Department of Civil Engineering, University of Minho, Campus Azurém, 4800-058 Guimarães, Portugal. L. G. Picado-Santos, Department of Civil Engineering, Foundation for Science and Technology, University of Coimbra, Polo 2, 3030 Coimbra, Portugal.

Transportation Research Record: Journal of the Transportation Research Board, No. 1919, Transportation Research Board of the National Academies, Washington, D.C., 2005, pp. 96–110.

slow and provides information about temperatures in the observed period only. Conversely, a temperature theoretical model may suffer slightly because of a lack of accuracies but will give a temperature distribution quickly and cheaply and can be used to predict temperature distributions under a wide range of conditions, including any unusual or extreme conditions.

The simulation model suggested in this paper is based on the finite element (FE) method, which involves weather data as input. The simulation model was validated by comparing the calculated temperatures with measured pavement temperatures obtained from December 2003 to April 2004. The model computes the pavement temperatures by using measured climate data values as input for the same time period.

Although this thermal approach may have the nature of a one-dimensional problem of the heat conduction in the vertical direction, given the infinite nature in the horizontal direction, the suggested model was developed on a 3D basis, having in view its future compatibility with a 3D mechanical reflective cracking model used by the authors in other projects.

BACKGROUND

To develop the pavement temperatures prediction model, basic principles needed to be adopted. The following sections present the main principles adopted in the proposed model once the hourly temperature distribution was governed by heat conduction principles within pavement and by energy interaction between the pavement and its surroundings.

Conduction Heat Transfer

Conjugating the first law of thermodynamics, which states that thermal energy is conserved, and Fourier's law, which relates the heat flux with the thermal gradient, the problem of heat transfer by conduction within the pavement is solved. For an isotropic medium and for constant thermal conductivity, this adopted principle is expressed as follows (*5*, *6*):

$$\nabla^2 T = \frac{1}{\alpha} \times \left(\frac{\partial T}{\partial t}\right) \tag{1}$$

where

$\nabla^2 = (\partial^2/\partial x^2) + (\partial^2/\partial y^2) + (\partial^2/\partial z^2)$,
$\alpha = \frac{k}{\rho \times C}$ = thermal diffusivity,
k = thermal conductivity,
ρ = density,
C = specific heat,
T = temperature,
t = time, and
x, y, and z = components of the Cartesian coordinate system.

Interaction Between Pavement and Surroundings

On a sunny day, the heat transfer by energy interaction between the pavement and its surroundings consists of radiation balance and exchanges by convection. The radiation balance (or thermal radiation) involves the consideration of outgoing longwave radiation, longwave counterradiation, and shortwave radiation (or solar radiation) (*7*).

The earth surface is assumed to emit longwave radiation as a black body. Thus, the outgoing longwave radiation follows the Stefan–Boltzman law (*5*, *7*):

$$q_e = \epsilon_e \sigma T_{sur}^4 \tag{2}$$

where

q_e = outgoing radiation,
ϵ_e = emission coefficient,
σ = Stefan–Boltzman constant, and
T_{sur} = pavement surface temperature.

As the atmosphere absorbs radiation and emits it as longwave radiation to the earth, this counterradiation absorbed by the pavement surface is calculated as proposed by Hermansson (*7*) and Dewitt and Incropera (*5*):

$$q_a = \epsilon_a \sigma T_{air}^4 \tag{3}$$

where

q_a = absorbed counterradiation,
ϵ_a = pavement surface absorptivity for longwave radiation and the amount of clouds, and
T_{air} = air temperature.

Several authors (*4*, *8*) consider the longwave radiation intensity balance (or thermal radiation) through the following expression:

$$q_r = h_r(T_{sur} - T_{air}) \tag{4}$$

where q_r is longwave radiation intensity balance, and h_r is the thermal radiation coefficient. The expression used to obtain h_r is as follows (*4*):

$$h_r = \epsilon\sigma(T_{sur} + T_{air})(T_{sur}^2 + T_{air}^2) \tag{5}$$

where ϵ is the emissivity of the pavement surface.

Part of the high-frequency (shortwave) radiation emitted by the sun is diffusely scattered in the atmosphere of the earth in all directions, and the diffuse radiation that reaches the earth is called diffused incident radiation. The radiation from the sun reaching the earth surface, without being reflected by clouds or absorbed or scattered by atmosphere, is called direct incident shortwave radiation. The total incident radiation (direct and diffused) can be estimated using the following equation (*4*–*6*):

$$q_i = \eta s_c f \cos\theta \tag{6}$$

where

q_i = thermal incident solar radiation,
η = loss factor accounting for scattering and absorption of shortwave radiation by atmosphere,
s_c = solar constant, assumed to be 1,353 W/m^2,
f = factor accounting for the eccentricity of earth orbit, and
θ = zenith angle.

The effective incident solar radiation absorbed by pavement surface may be determined by the following equation (*8*):

$$q_s = \alpha_s \times q_i \tag{7}$$

where q_s is the incident solar radiation absorbed by the pavement surface and α_s is the solar radiation absorption coefficient.

In the model suggested in this paper, shortwave radiation is given as input data obtained measured values. The convection heat transfer between the pavement surface, and the air immediately above is given as follows (*4, 7*):

$$q_c = h_c(T_{sur} - T_{air}) \tag{8}$$

where q_c is convection heat transfer and h_c is the convection heat transfer coefficient. The convection heat transfer coefficient can be calculated as follows:

$$h_c = 698.24\{[1.44 \times 10^{-3} T_{ave}^{0.3} U^{0.7}] + [9.7 \times 10^{-4}(T_{sur} - T_{air})^{0.3}]\}$$

where T_{ave} is the average temperature given by $T_{ave} = (T_{sur} - T_{air})/2$ and U is the wind speed.

FINITE DIFFERENCE METHODOLOGY

The transient temperature response of pavements may be analyzed through a numerical incremental recursive model, using the finite differences method, by applying the energy balance principle and the Fourier heat transfer equation. The thermal conductivity and thermal diffusivity of pavement are estimated through a convergence process.

The discrete form of Fourier equations within the layer can be written as follows (*4*):

$$K_i\left(\frac{T_{m-1}^p - T_m^p}{\Delta z}\right) - K_i\left(\frac{T_m^p - T_{m+1}^p}{\Delta z}\right) = \rho C\left(\frac{T_m^{p+1} - T_m^p}{\Delta t}\right)\Delta z \tag{9}$$

where

- Δt = time increment;
- Δz = depth increment;
- p = time superscript, such that $|T^{p+1} - T^p| = \Delta t$;
- m = depth subscript, such that $|z_{m+1} - z_m| = \Delta z$;
- K_i = thermal conductivity coefficient of layer i; and
- T_m^p = temperature in the node m at time p.

The discrete form of Fourier equations in the interface zone of layers can be written as follows (*4*):

$$T_m^{p+1} = \frac{2\Delta t}{r(\Delta z)^2}\left(K_i + T_{m+1}^p + K_{i+1}T_{m-1}^p\right) + \left[1 - \frac{2K_i\Delta t}{r(\Delta z)^2} - \frac{2K_{i+1}\Delta t}{r(\Delta z)^2}\right]T_m^p \tag{10}$$

where $r = C_i\rho_i + C_{i+1}\rho_{i+1}$. Interaction between the pavement and its surroundings at surface ($z = 0$) can be written as follows (*4*):

$$h_r(T_{air} - T_{sur}^p) + q_s + h_c(T_{air} - T_{sur}^p) + K_i\left(\frac{T_1^p - T_{sur}^p}{\Delta z}\right) = \rho C\frac{\Delta z}{2}\left(\frac{T_{sur}^{p+1} - T_{sur}^p}{\Delta t}\right) \tag{11}$$

An Excel spreadsheet was developed to solve the transient state temperature model using the finite differences method. The equations were solved incrementally at each 30-s time step to predict temperature at any given depth at a given time step. The model solution requires the determination of initial temperature distribution in the layer system before transient analysis. The initial temperature distribution adopted was obtained from field measurements.

FE METHOD

This study is based on the use of the FE method in the prediction of temperature distributions in AC pavements. In the last several years, this methodology has been revealed to be a tool of great applicability in the pavement research domain.

Conduction

The first law of thermodynamics, which states that thermal energy is conserved, was used to build the solution of the pavement thermal problem through FEs. Considering a differential control volume of a pavement, in that methodology, the conservation of thermal energy is expressed by Equation 12:

$$\rho C\frac{\partial T}{\partial t} + \{L\}^T\{q\} = 0 \tag{12}$$

where

T = temperature = $T(x, y, z, t)$,

$$\{L\} = \begin{Bmatrix} \partial/\partial x \\ \partial/\partial y \\ \partial/\partial z \end{Bmatrix} = \text{vector operator, and}$$

$\{q\}$ = heat flux vector.

The term $\{L\}^T\{q\}$ also may be interpreted as $\nabla \times \{q\}$, where ∇ represents the divergence operator. Fourier's law can be used to relate the heat flux vector to the thermal gradients through the following expression:

$$\{q\} = -[D]\{L\}T \tag{13}$$

where

$$[D] = \begin{bmatrix} K_{xx} & 0 & 0 \\ 0 & K_{yy} & 0 \\ 0 & 0 & K_{zz} \end{bmatrix}$$

is the conductivity matrix and K_{xx}, K_{yy}, K_{zz} are the thermal conductivity in the element x, y, and z directions, respectively.

Expanding equation to its more familiar form gives the following:

$$\rho C\frac{\partial T}{\partial t} = \frac{\partial}{\partial x}\left(K_{xx}\frac{\partial T}{\partial x}\right) + \frac{\partial}{\partial x}\left(K_{yy}\frac{\partial T}{\partial y}\right) + \frac{\partial}{\partial x}\left(K_{zz}\frac{\partial T}{\partial z}\right) \tag{14}$$

Considering the isotropy of material ($K = K_{xx} = K_{yy} = K_{zz}$) yields the following:

$$\rho C\frac{\partial T}{\partial t} = \frac{\partial}{\partial x}K\left[\left(\frac{\partial T}{\partial x}\right) + \frac{\partial}{\partial x}\left(\frac{\partial T}{\partial y}\right) + \frac{\partial}{\partial x}\left(\frac{\partial T}{\partial z}\right)\right] \tag{15}$$

Boundary Conditions

Three types of boundary conditions, which cover the entire model, were considered: heat flow acting over the model surface limits, surface convection applied in the superior surface of model, and the radiant energy between the model superior surface and its surroundings.

Specified heat flow acting over a surface follows the general expression shown in Equation 16:

$$\{q\}^T\{\eta\} = -q^* \quad (16)$$

where $\{\eta\}$ is the unit outward normal vector and q^* is the specified heat flow.

Specified convection-surfaces heat flows acting over a surface follows the general expression shown in Equation 17:

$$\{q\}^T\{\eta\} = h_f(T_{sur} - T_{air}) \quad (17)$$

where

h_f = convection coefficient,
T_{sur} = temperature at the surface of the model, and
T_{air} = bulk temperature of the adjacent fluid.

Radiant energy exchange between a surface of the model and its surroundings is translated by the following expression, which gives the heat transfer rate between the surface and a point representing the surroundings:

$$q_r = \sigma\varepsilon(T_{sur}^4 - T_{air}^4) \quad (18)$$

3D FE METHOD PAVEMENT THERMAL MODEL

The 3D FE method (FEM) was used to model the thermal behavior of pavement. The pavement structures traditionally are idealized as a set of horizontal layers of constant thickness; homogeneous, continuous, and infinite in the horizontal direction; resting on a subgrade; and semi-infinite in the vertical direction. The thermal configuration of the pavement model was defined based on those principles and is presented in Figure 1. This model considers the possibility of data production for a mechanical model with the same mesh.

The adopted mesh also has been designed for study of the reflective cracking phenomenon caused by the traffic loading and represents an existing pavement, in which a crack is simulated through an element with zero-stiffness and a layer on top of the existing pavement represents an overlay. This mesh was described in other works by the authors (*9*).

The FEM used in numerical thermal analysis was performed using a general FEs analysis source code, ANSYS 5.6 (*10*). This analysis is a 3D transient analysis, using a standard FE discretization of the pavement. In the design of the thermal FE mesh, the compatibility of mesh with other mechanical models was observed.

The following factors have been considered in the design of the FE mesh:

- A finer element size is adopted closer to the pavement surface and closer to the wheel load zone, where stress gradient may be highest.

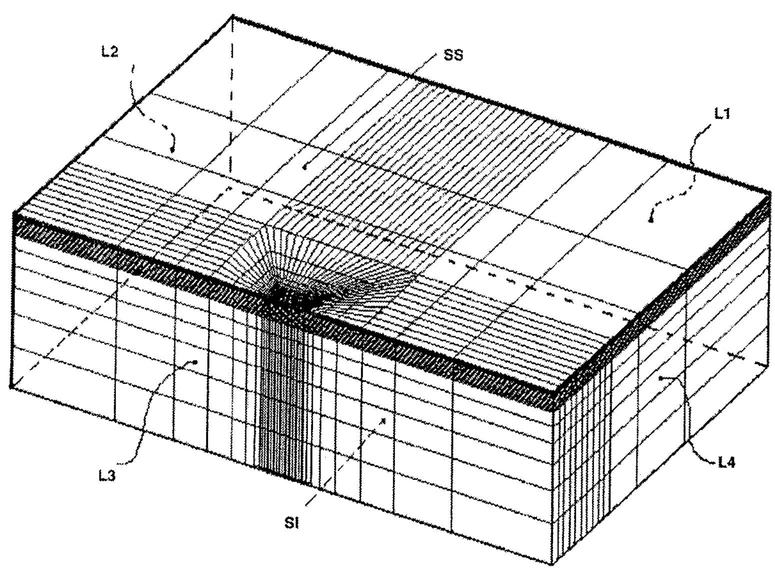

FIGURE 1 FEM mesh thermal model (L1–L4 and SI are boundary surfaces of model and SS represents pavement surface).

- A finer element size is required in the overlay above the crack.
- Because of the symmetry, only half of the model needs to be modeled, which reduces the time consumed in the computing process.

After designed mesh, the number of elements was 13,538. For 3D thermal analysis, a 3D solid element, SOLID70, was used (Figure 2). This element (applicable to a 3D transient thermal analysis) has the capability for 3D thermal conduction, according to the previous explanation. The element has eight nodes with a single degree of freedom (temperature) at each node.

The thermal properties of pavement material (e.g., thermal conductivity, specific heat, and density) for each pavement layer were defined in the "material properties" of this element, when the model was developed. For surface effect applications, such as radiation exchanges by convection heat transfer, the surface element SURF152 was used. The geometry, node locations, and the system coordinates for this element are shown in Figure 3.

The element is defined by four nodes and by material properties. An extra node (away from the base element) is used to simulate the effects of convection and radiation and represents the point where the hourly air temperature is introduced (representing the atmosphere). It was overlaid onto an area face of 3D thermal element SOLID70, as shown in Figure 4. The element is applicable to 3D thermal analysis and allows these load types and surface effects, such as heat fluxes, to exist simultaneously. The surface elements were placed on the entire surface SS (Figure 1).

The convection coefficient (or film coefficient) must be used to consider surface convection in the conductivity matrix calculation. When an extra node is used, its temperature becomes the air temperature. This element allows for radiation between the surface and the extra node "M." The emissivity of the surface is used for the conductivity matrix calculation, for considering surface radiation, and the Stefan–Boltzman constant is used for the conductivity matrix calculation.

The solar radiation is considered as a heat flux that is applied on surface SS. To define the boundary conditions, a null heat flux is applied on surfaces L1, L2, L3, L4, and SI, presented in Figure 1.

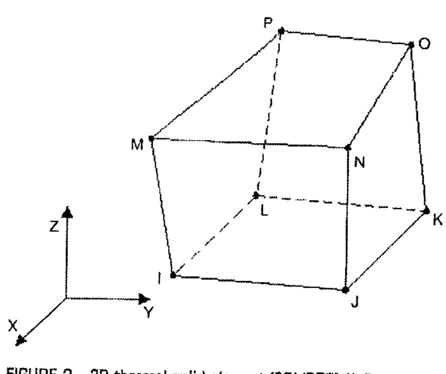

FIGURE 2 3D thermal solid element (SOLID70) (I–P are element nodes).

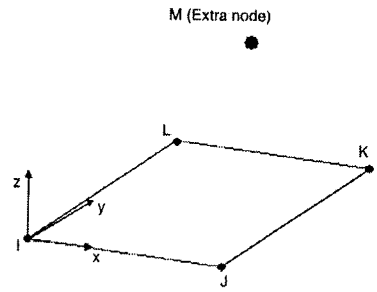

FIGURE 3 Surface thermal element (SURF152) (I–M are element nodes).

PAVEMENT TEMPERATURE PREDICTION—CASE STUDY

The main goal of this study was to validate an FEM simulation model developed to calculate the temperatures of a pavement. A FEM numerical analysis for the distribution of temperature in a full-depth asphalt pavement in a trial section located on km 197.700 of IP4 (Bragança, Portugal) was performed for the weather conditions (air temperature, solar radiation, and wind speed) from December 2003 to June 2004.

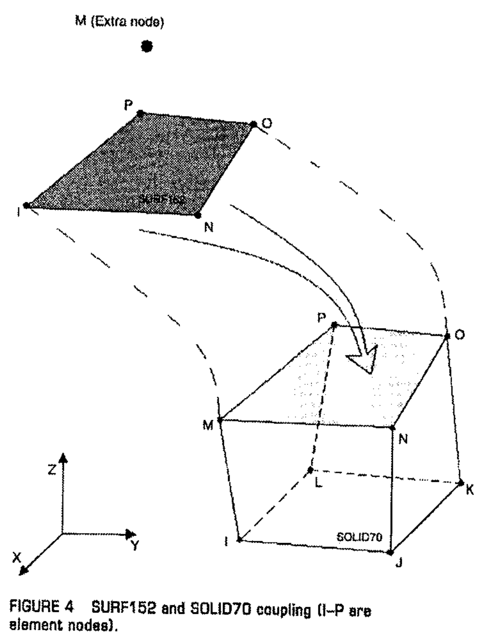

FIGURE 4 SURF152 and SOLID70 coupling (I–P are element nodes).

The model validation was made by statistical analysis between the FEM numerical temperature results, finite differences temperature results, and the field-measured temperatures.

Field Data Collection

For 4 months (December 2003 to April 2004), pavement temperatures were measured at a new pavement section, located at IP4 main road, near from Bragança, in the north of Portugal. At that location, seven thermocouples were installed in the AC layer at seven different depths: 0, 27.5, 55, 125, 165, 220, and 340 mm. The top thermocouple was installed just at the pavement surface. The depths for the other six were chosen to give a good representation of the whole AC layers at different locations. AC temperatures were recorded every hour of every day.

With respect to short-term temperature response, it can be argued that subgrade temperature at 2.0-m depth is reasonably constant over a given month. The hourly measurements of weather parameters, such as air temperature, solar radiation intensity, and wind speed, were obtained from a meteorological station located near the test pavement section. These measurements were used as input data in the simulation models to carry out temperature distribution prediction in a 340-mm full-depth pavement.

Input Data to Simulation

The pavement surface thermal emissivity for estimating the long-wave radiation intensity balance was equal to 0.9, and the solar absorption coefficient was equal to 0.95. Table 1 presents the values for the pavement material thermal properties adopted in this study. The parameters have been adapted to give a good correspondence between calculated and measured pavement temperatures. The adopted values follow the typical values for those parameters suggested by previous research (*2–4, 7*).

As expressed in the conclusions obtained from a simulation made by Hermansson (*7*), the influence of the thermal conductivity of the pavement is marginal for the pavement temperatures close to the surface. Thus, no further effort was made in this paper to study the influence of thermal conductivity variation.

Analysis Procedure

The thermal response of the FEM simulation model, representing a multilayered pavement structure, was modeled using a transient thermal analysis for 4 months (from December 2003 to April 2004). This is the best period (winter) of analysis to study the reflective cracking phenomenon, subjected to influence of temperature variations. It was assumed that the pavement hourly temperature profile depended entirely on hourly air temperature value, hourly solar radiation value, and wind speed daily mean value.

The analysis procedure involved multiple 3D FE runs and was initiated with the full depth at constant initial temperature, obtained from field measurements. The analysis procedure was carried out for a period between December 2003 and April 2004, with a periodicity of 1 h. The thermal response analysis performed by the finite differences method was made for the same conditions used in the finite element method.

RESULTS

As a measure of error, the absolute difference between calculated and measured pavement temperatures was calculated for every hour. Then the average difference was determined for each month and for the total time period, which is assigned as average error. Table 2 presents the result of this procedure, and Table 3 presents the standard deviation of errors. Figures 5 to 11 present the temperature distributions in the months of January and April 2004, located at surface, 55-mm depth, and 165-mm depth, and March for 55-mm depth where a good correlation was obtained between the in situ measurements and the calculated temperature.

CONCLUSIONS

The 3D FE analysis has proved to be an interesting tool to simulate the transient behavior of asphalt concrete pavement temperature. According to comparisons performed with field measurements, the suggested simulation model can model the pavement temperature at different levels of bituminous layers with good accuracy. To obtain this distribution, a series of climatic data is needed as an input to the model. The use of the results for other FEM mechanical models constitutes a great advantage of the proposed model.

In comparison of measured and calculated temperature data for every hour for 4 months, an average error less than 2.1°C was obtained in the depths close to the surface. At a depth of 340 mm, the average error may reach 4°C in April. In cold months, the average error is less than in hot months. Thus, in the cold months, the developed model presents better performance than in hot months.

The average error produced by the FEM simulation model is closer to the average error produced by finite difference methodology. The small error variations observed between these models can be caused by the consideration of the average wind speed in FEM model. The

TABLE 1 Layer Thermal Properties

	Thickness (m)	K (W/°C.m)	C (W.s/kg.°C)	Density (kg/m^3)
Overlay—wearing course	0.055	1.5	850	2550
Overlay—base course	0.070	1.5	860	2350
Cracked layer	0.215	1.5	850	2550
Subbase	0.300	1.5	805	2370
Subgrade	—	1.79	1100	2200

TABLE 2 Average Error Results

	Average Errors (degree C)													
Depth >	0 mm		27.5 mm		55 mm		125 mm		165 mm		220 mm		340 mm	
Month Method >	Fin. Diff.	FEM	Fin. Diff.	FEM	Fin. Diff.	FEM	Fin. Diff.	FEM	Fin. Diff.	FEM	Fin. Diff.	FEM	Fin. Diff.	FEM
December	1.7305	2.1892	1.5251	1.9867	1.3084	1.7164	1.1059	1.3043	1.184	1.0978	1.4373	0.9521	2.6714	2.1224
January	1.6697	1.6985	1.4632	1.5323	1.3639	1.3754	1.2304	1.1993	0.9665	0.9327	0.7856	0.7229	1.7828	1.9414
February	1.3608	1.3675	1.1767	1.2076	1.062	1.0318	0.7143	0.7055	1.0661	0.9145	0.7122	0.6951	2.613	2.4323
March	1.3604	1.3878	1.1726	1.2091	1.2069	1.179	1.5942	1.3959	1.8198	1.4972	1.0481	0.8016	2.8134	2.647
April	2.0394	2.0085	1.9417	2.0141	1.7611	1.6663	2.0518	1.8459	2.2845	1.9264	1.4738	1.2073	4.2292	4.0886
December–April	1.6441	1.6825	1.4745	1.5572	1.3719	1.3665	1.4168	1.3238	1.5311	1.3234	1.0538	0.8773	2.8677	2.7632

NOTE: Fin. Diff. = finite differences.

TABLE 3 Standard Deviation of Error Results

	Standard Deviation of Errors (degree C)													
Depth >	0 mm		27.5 mm		55 mm		125 mm		165 mm		220 mm		340 mm	
Month Method >	Fin. Diff.	FEM	Fin. Diff.	FEM	Fin. Diff.	FEM	Fin. Diff.	FEM	Fin. Diff.	FEM	Fin. Diff.	FEM	Fin. Diff.	FEM
December	1.1553	1.5899	0.9263	1.3457	0.9026	1.0678	0.9149	0.7346	0.9236	0.6562	0.6885	0.64	1.6151	1.0578
January	1.3382	1.3795	1.202	1.2571	1.0186	1.0798	0.8126	0.8333	0.6854	0.7742	0.5209	0.6305	1.3446	1.1094
February	1.0773	1.0843	0.82	0.8782	0.7761	0.7716	0.5463	0.5452	0.7522	0.6973	0.5073	0.4846	1.7641	1.4332
March	1.2977	1.3246	0.9796	1.0594	1.0747	1.0601	1.1578	1.1019	1.3582	1.1674	0.9383	0.8001	2.1728	2.0396
April	1.6421	1.6259	1.312	1.3569	1.2859	1.2365	1.3	1.2326	1.7471	1.4497	0.8732	0.7271	2.8718	2.6089
December–April	1.3871	1.4314	1.1469	1.2349	1.0899	1.0955	1.1144	1.0416	1.3367	1.1404	0.8002	0.7045	2.2874	2.0395

NOTE: Fin. Diff. = finite differences.

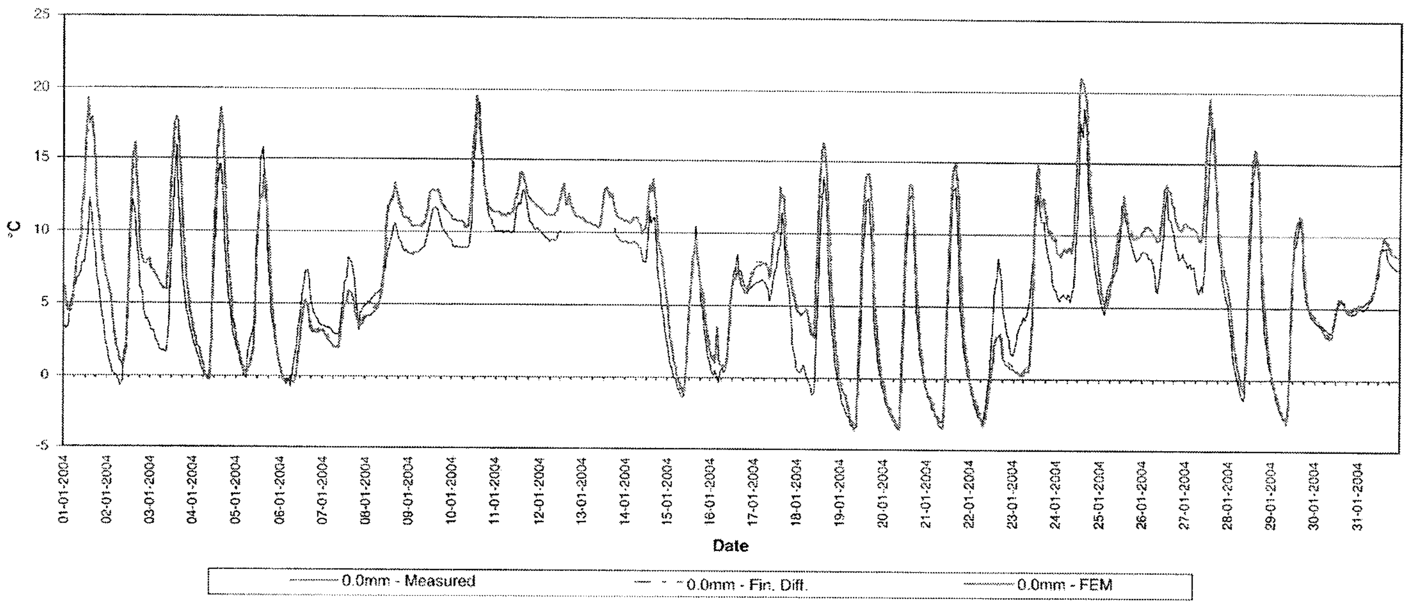

FIGURE 5 January 0.0-mm depth temperature distribution (Fin. Diff. = finite differences method).

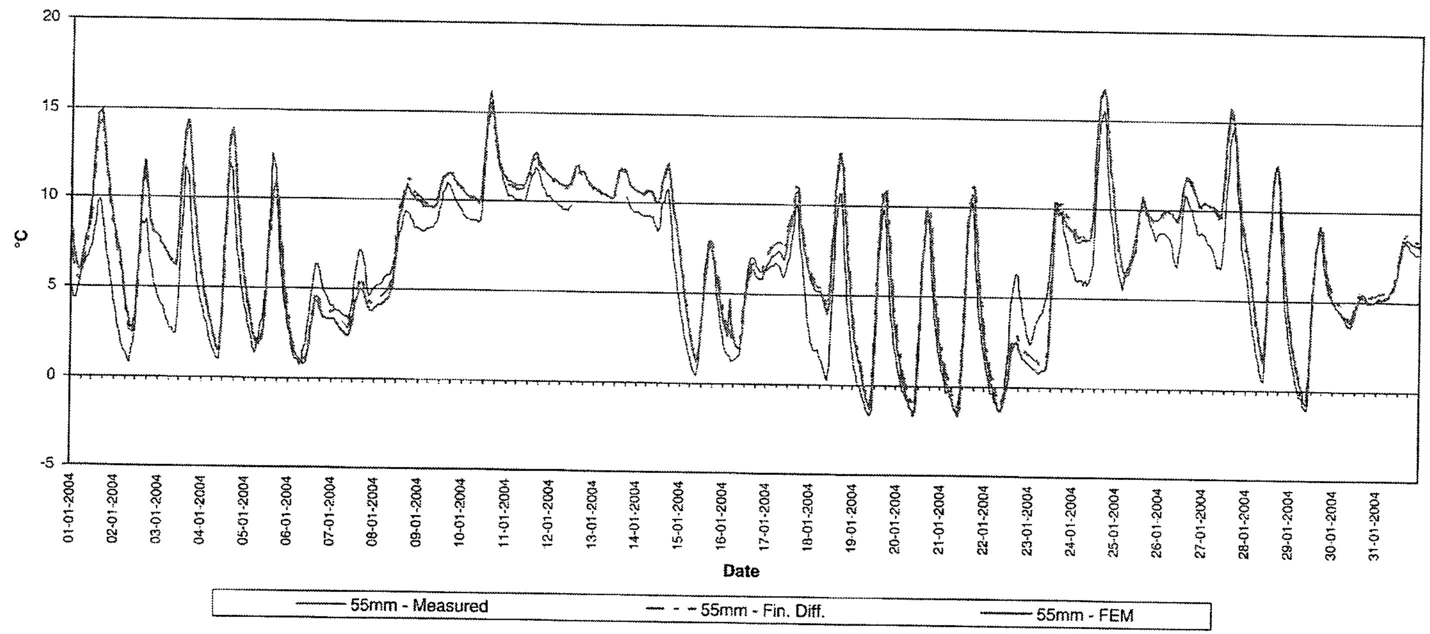

FIGURE 6 January 55-mm depth temperature distribution (Fin. Diff. = finite differences method).

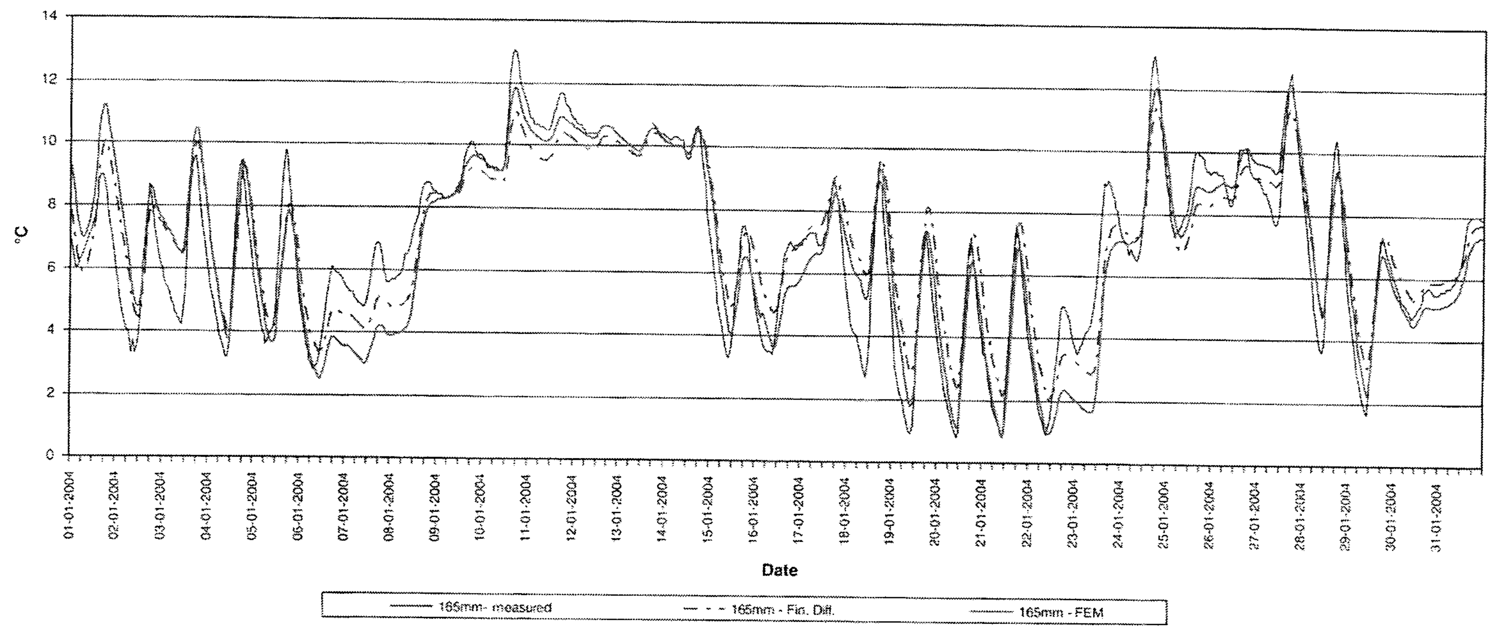

FIGURE 7 January 165-mm depth temperature distribution (Fin. Diff. = finite differences method).

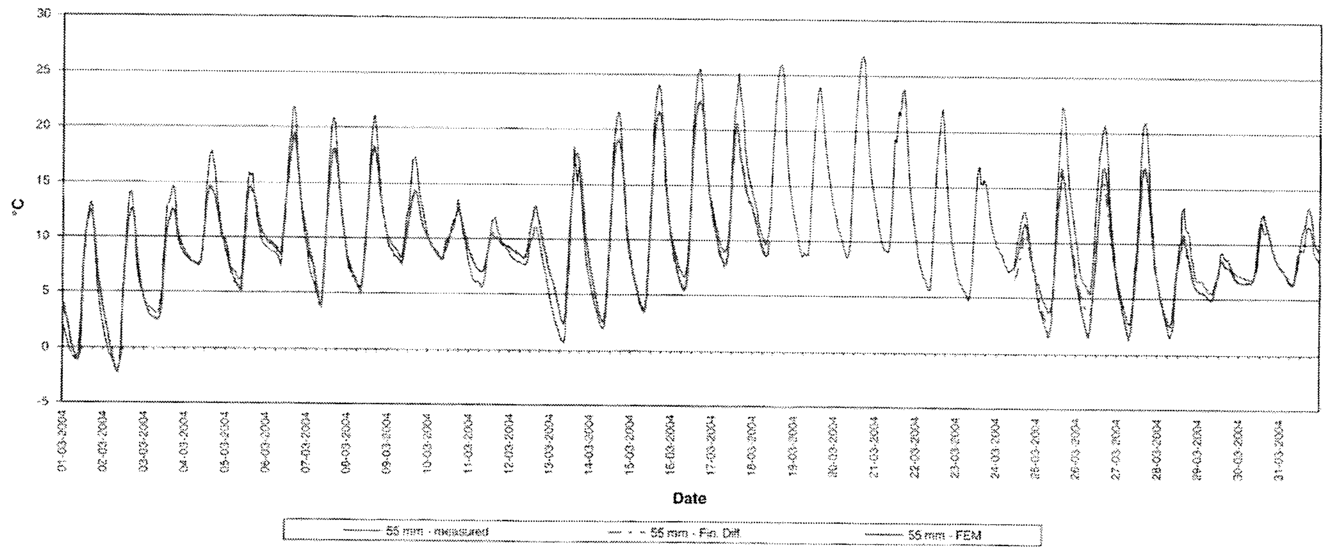

FIGURE 8 March 55-mm depth temperature distribution (Fin. Diff. = finite differences method).

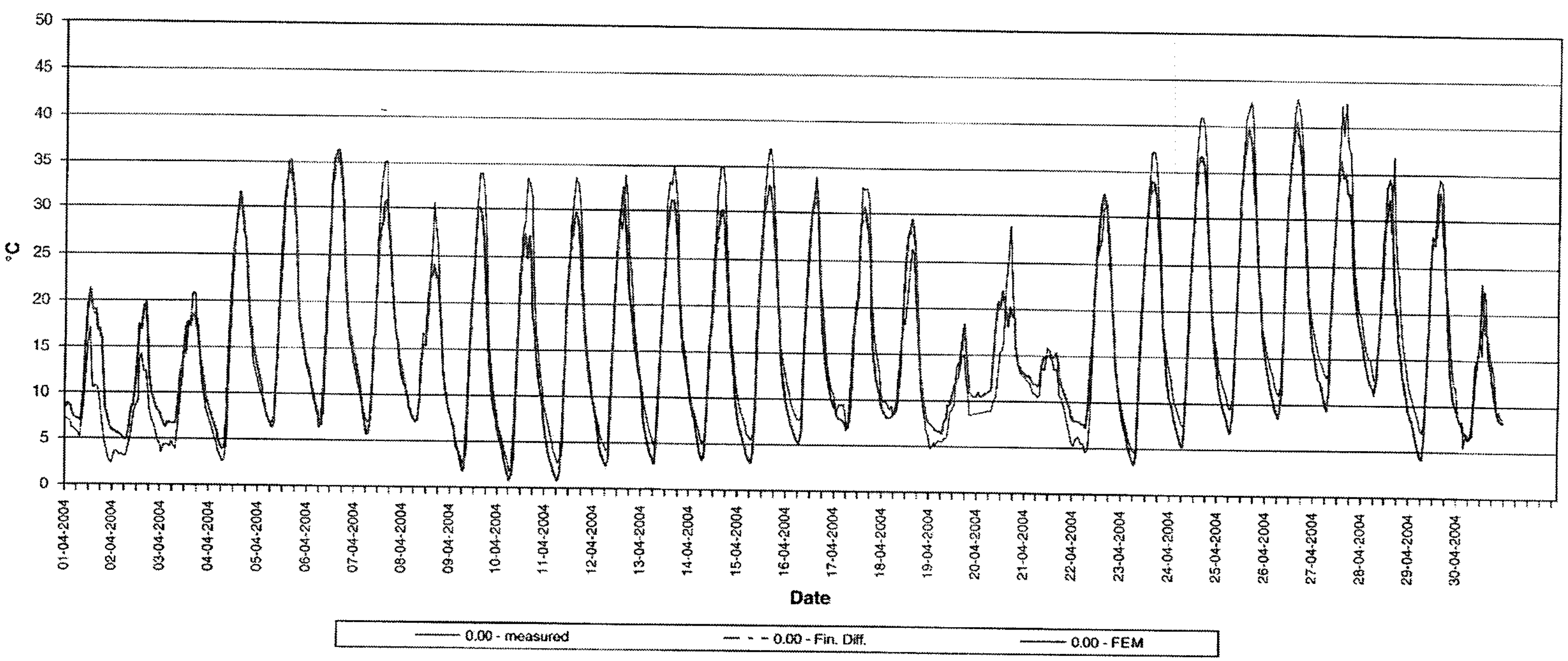

FIGURE 9 April 0.0-mm depth temperature distribution (Fin. Diff. = finite differences method).

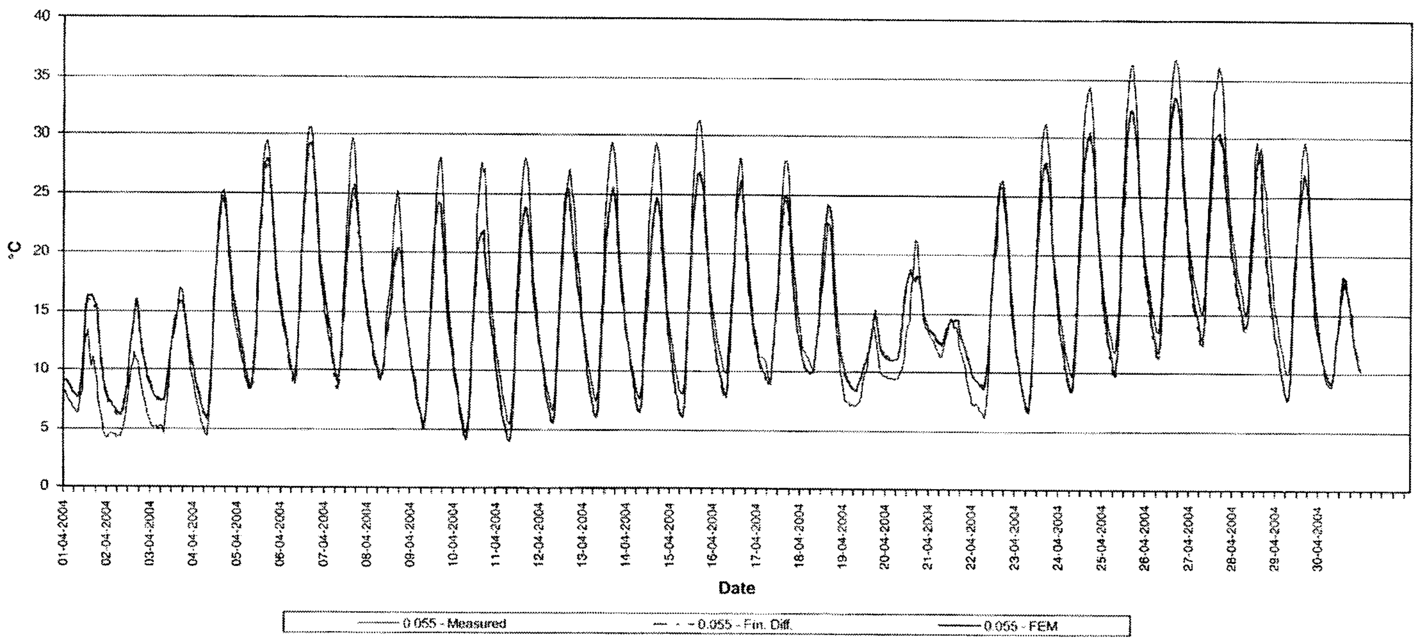

FIGURE 10 April 55-mm depth temperature distribution (Fin. Diff. = finite differences method).

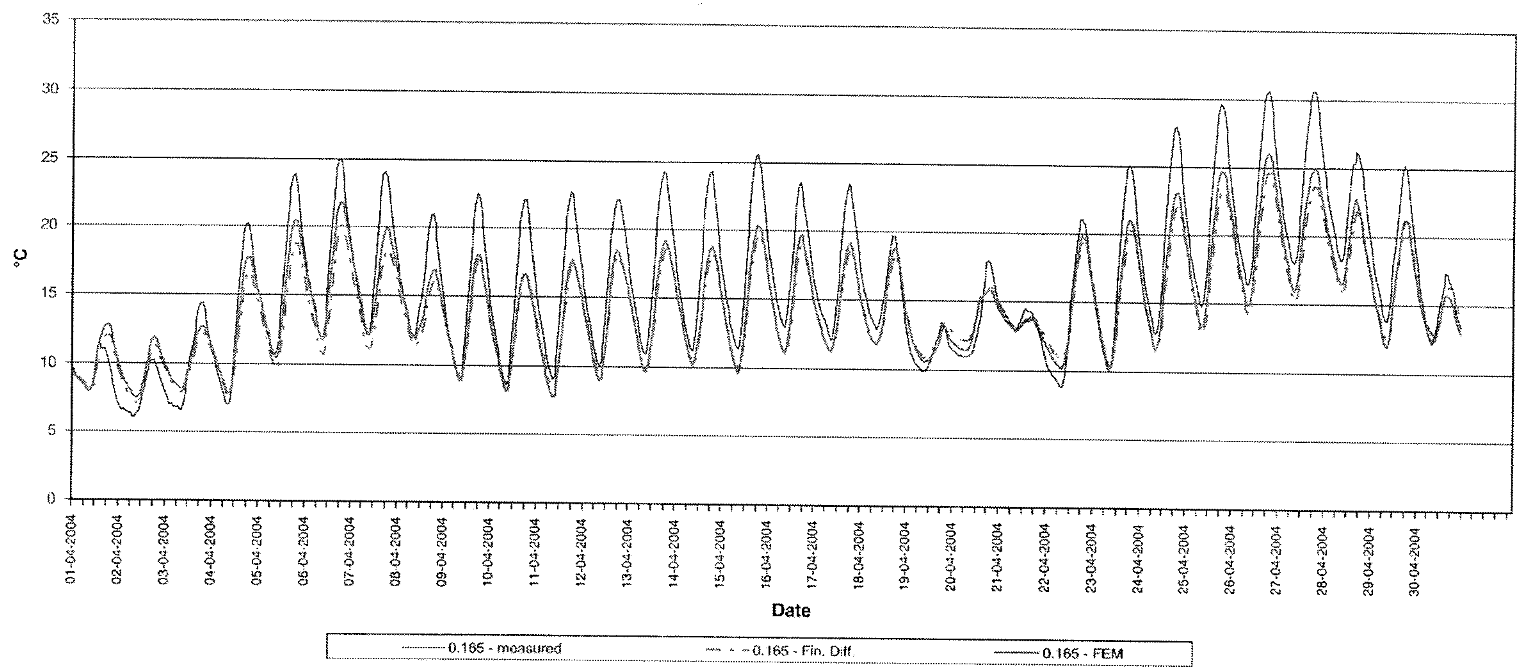

FIGURE 11 April 165-mm depth temperature distribution (Fin. Diff. = finite differences method).

3D FEM model also produces good results when compared with models of one-dimensional nature.

ACKNOWLEDGMENT

The authors acknowledge the work and technical support from the Bragança delegation of the Portuguese Road Administration.

REFERENCES

1. Sousa, J. B., J. C. Pais, R. Saim, G. B. Way, and R. N. Stubstad. Mechanistic–Empirical Overlay Design Method for Reflective Cracking. In *Transportation Research Record: Journal of the Transportation Research Board, No. 1809*, Transportation Research Board of the National Academies, Washington, D.C., 2002, pp. 209–217.
2. de Bondt, A. Effect of Reinforcement Properties. *Proc., PRO11 4th International RILEM Conference on Reflective Cracking in Pavements—Research in Practice* (A. O. Abd Halim, D. A. Taylor, and H. H. Mohamed, ed.), RILEM, Ottawa, Ontario, Canada, 2000, pp. 13–22.
3. Shalaby, A., A. O. Abd El Halim, and S. M. Easa. Low-Temperature Stresses and Fracture Analysis of Asphalt Overlays. In *Transportation Research Record 1539*, TRB, National Research Council, Washington, D.C., 1996, pp. 132–139.
4. Mrawira, D. M., and J. Luca. Thermal Properties and Transient Temperature Response of Full-Depth Asphalt Pavements. In *Transportation Research Record: Journal of the Transportation Research Board No. 1809*, Transportation Research Board of the National Academies, Washington, D.C., 2002, pp. 160–169.
5. Dewitt, D. P., and F. P. Incropera. *Fundamentals of Heat and Mass Transfer*. 4th ed. John Wiley and Sons, New York, 1996.
6. Özisik, M. N. *Heat Transfer: A Basic Approach*. McGraw-Hill, New York, 1985
7. Hermansson A. Mathematical Model for Calculation of Pavement Temperatures: Comparisons of Calculated and Measured Temperatures. In *Transportation Research Record: Journal of the Transportation Research Board, No. 1764*, TRB, National Research Council, Washington, D.C., 2001, pp. 180–188.
8. Picado-Santos, L. *Consideração da Temperatura no Dimensionamento de Pavimentos Rodoviários Flexíveis* [in Portuguese]. Ph.D. thesis. University of Coimbra, Lisbon, Portugal, 1994.
9. Minhoto, M. J. C., J. C. Pais, P. A. A. Pereira, and L. G. Picado-Santos. Low-Temperature Influence in the Predicted Pavement Overlay Life. Presented at Asphalt Rubber 2003 Conference, Brasilia, Brasil, 2003, pp. 167–180.
10. ANSYS 5.6 [computer program]. ANSYS Theory Reference—Realise 5.6. Edited by Peter Kohnke. ANSYS, Inc., Canonsburg, Pa., 1999.

The Flexible Pavement Design Committee sponsored publication of this paper.